A Weakly-Coupled Few-Mode Hybrid Clad Photonic Crystal Fiber With Ultra-Flattened Dispersion and Low Confinement Loss

Xiao Lei, Fang Ren, Yanfei Zhang, Yingjuan Ci, Xiaohui Wang, and Jianping Wang

***Abstract*—We propose a weakly-coupled ultra-flattened chromatic dispersion few-mode photonic crystal fiber (FM-PCF) supporting 10 vector modes (HE_{11a}, HE_{11b}, TM_{01}, HE_{21a}, HE_{21b}, TE_{01}, HE_{31a}, HE_{31b}, EH_{11a}, EH_{11b}) which works over a large range of wavelength across the C+L band. We investigate the chromatic dispersion, minimum effective refractive index difference ($\min\Delta n_{eff}$), confinement loss, bending loss and differential mode delay (DMD) of the proposed fiber under the influences of design parameters by using the finite element method (FEM). The circular holes in the first ring are replaced by elliptical holes to obtain flattened-chromatic dispersion. And an extra small rectangular defected hole is introduced in the fiber core order to achieve ultra-flattened chromatic dispersion and large $\min\Delta n_{eff}$. The simulated results show that the designed weakly-coupled FM-PCF can obtain ultra-flattened (dispersion slope $< 1.8 \times 10^{-4}$ ns/km/nm^2) and large $\min\Delta n_{eff}$ ($> 1.6 \times 10^{-4}$) in the wavelength range of 1520 nm to 1640 nm. And the proposed weakly-coupled FM-PCF also has ultra-low confinement loss ($<10^{-9}$dB/km) and good bending resistance. In summary, the proposed weakly-coupled FM-PCF has the potential applications for large-capacity MDM communication systems.**

***Index Terms*—Photonic crystal fiber, chromatic dispersion, dispersion slope, confinement loss, few modes fiber.**

I. Introduction

PHOTONIC crystal fibers (PCFs) intrigue many researchers due to the high flexibility of design and some unique optical properties, such as the endlessly single mode, high nonlinearity, high birefringence and ultra-flatten dispersion [1], [2], [3], [4], [5]. Therefore, PCFs can be used for many potential applications in telecommunications [6], sensing [7], non-linear optics [8] and other fiber devices. However, with the exponentially growing demand on communication capacity of signal transmission systems, to further increase the capacity of transmission media has become an urgent need [9]. In recent years, several techniques such as time-division multiplexing [10], polarization division multiplexing [11], and wavelength division multiplexing [12] used to improve the transmission capacity of optical fibers. However, single mode fiber, is rapidly approaching its capacity limit due to the nonlinear Shannon effect [13], [14]. Therefore, space division multiplexing (SDM) technology based on PCF has become a new focus, which is expected to expand the transmission capacity and realize the flat dispersion transmission of few modes.

Dispersion control plays a critical role in optical communication, and photonic crystal fiber with flattened chromatic dispersion have been the target of many researchers in the last few years. In order to achieve flattened chromatic dispersion, two main ways are adopted: firstly, by the arrangement of air holes in cladding, lattice geometry size and shape of the holes, there is possibilities to control light propagation, such as triangular, rectangular, octagonal and equiangular spiral structure [15], [16], [17], [18]. Another way is to add additional materials, either by doping the core with high index materials such as germanium [19]and fluorine [20], or by infiltrating low index fluids into selected air holes [21]. However, using additional materials undoubtedly increase the difficulties in the manufacturing process. In recent years, many photonic crystal fibers with flattened chromatic dispersion have been proposed. For example, Zhang [22] proposed a novel photonic crystal fiber, which is composed of a solid silica core and a cladding with square lattice uniform elliptical air holes and has flattened chromatic dispersion (±2.5 ps/nm/km). Animesh et al. [1] designed a circular-lattice photonic crystal fiber which has ultra-flattened average dispersion of −124.0 ps/(nm.km) with a dispersion variation of ± 0.1252 ps/(nm.km) and low confinement loss. Wang et al. [23] proposed a new photonic crystal fiber with D-sharped air holes in the core region, which has a flattened dispersion of 0.09 ± 0.28 ps/THz/cm and low confinement loss. However, these photonic crystal fibers only support single fundamental mode, there are few reports on weakly-coupled few-mode photonic crystal fiber (FM-PCF). In recent years, Shi et al. [24] designed a few-mode photonic crystal fiber with special air holes, which has the flattened chromatic dispersion curve by removing part of the air holes in cladding. The designed fiber can achieve three vector mode dispersion flattening in the

Manuscript received 21 June 2022; revised 19 July 2022; accepted 26 August 2022. Date of publication 30 August 2022; date of current version 12 September 2022. This work was supported in part by the Fundamental Research Funds for the Central Universities under Grant FRF-BD-20-11A and in part by the State Key Laboratory of Advanced Optical Communication Systems Networks, Peking University, Beijing, China. *(Corresponding author: Fang Ren).*

The authors are with the School of Computer and Communication Engineering, University of Science and Technology Beijing, Beijing 100083, China, and also with the Beijing Engineering and Technology Research Center for Convergence Networks and Ubiquitous Services, University of Science and Technology Beijing, Beijing 100083, China (e-mail: leixiao1368405503@163.com; renfang@ustb.edu.cn; zyf-sd@foxmail.com; ciyingjuan@163.com; m202120777@xs.ustb.edu.cn; jpwang@ustb.edu.cn).

Digital Object Identifier 10.1109/JPHOT.2022.3202815

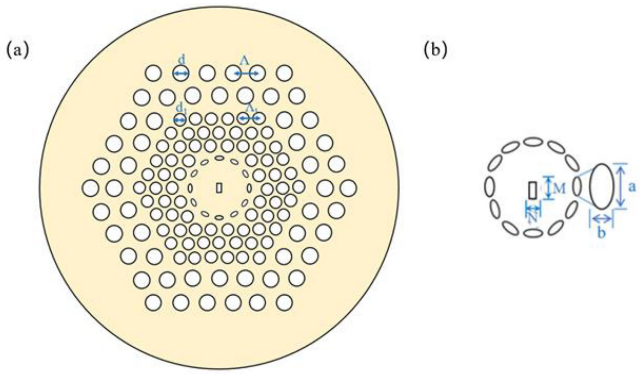

Fig. 1. Cross sectional view (a) and zoomed core region (b) of proposed weakly-coupled FM-PCF.

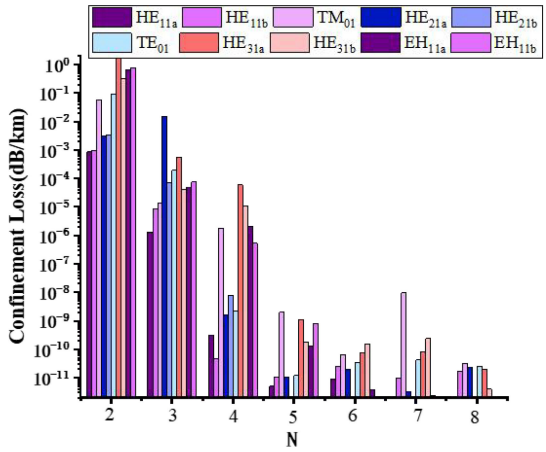

Fig. 2. Confinement losses of the proposed weakly-coupled FM-PCF versus the number N of air holes rings.

wavelength range of 1530 $\sim$ 1560 nm, but the confinement loss is large (>1dB/m), and the actual manufacturing will be difficult because of the complexity of fiber structure.

In this paper, we proposed the weakly-coupled FM-PCF supporting 10 vector modes, which has ultra-flattened dispersion (dispersion slope $< 1.8 \times 10^{-4}$ ns/km/nm2) and ultra-low confinement loss (<10−9 dB/km). The chromatic dispersion, minΔneff, effective mode area, bending loss and nonlinear coefficient of the proposed FM-PCF are investigated. To achieve ultra-flattened chromatic dispersion and large minΔneff, an extra small rectangular defected hole is introduced in the fiber core. The circular holes in the first ring are replaced by elliptical holes to further obtain flattened-chromatic dispersion. Simulation results show that the proposed weakly-coupled FM-PCF can support 10 vector modes and the minimum effective index difference (minΔneff) is larger than $1.6 \times 10-4$ over the whole C+L band, which can improve the utilization of vector modes and avoid the mode coupling between adjacent modes. The proposed weakly-coupled FM-PCF can meet the two advantages of low mode crosstalk and flat dispersion and can improve the communication capacity and communication quality of Mode Division Multiplexing communication systems. And the proposed weakly-coupled FM-PCF also has strong resistance bending sensitivity (the bending loss <10−4 dB/km), which has the potential applications for large-capacity MDM communication systems.

II. Geometry of the Proposed Fiber Structure

The weakly-coupled FM-FCF cross section and the enlarged view of the fiber core proposed in this paper are shown in Fig. 1. It is composed of five hexagonal rings of circular air holes and a circular ring of elliptical air holes. The distribution of air holes in the inner and outer rings of the cladding is different, which the outer holes are kept large to reduce the confinement loss and the inner hole size is scaled down in order to control the dispersion. The pitch and the diameters of the outer and inner cladding air holes are Λ, d, Λ_1 and d_1. The circular holes in the first ring are replaced by elliptical holes to obtain flattened-chromatic dispersion, and the diameter of the first ring holes are a and b. An extra defected rectangular air hole (with hole diameter M and N) is introduced in the center of fiber, which is apt to control dispersion and obtain the ultra-flattened chromatic dispersion. The proposed weakly-coupled FM-PCF characteristics are simulated with finite element method (FEM), the background material is silica and its refractive index is given by the Sellmeier equation [25],

$$n_{silica}(\lambda) = \sqrt{\frac{0.6961663\lambda^2}{\lambda^2-0.0684043^2} + \frac{0.4079426\lambda^2}{\lambda^2-0.1162414^2} + \frac{0.8974794\lambda^2}{\lambda^2-9.896161^2} + 1}, \quad (1)$$

where λ is the transmission wavelength.

III. Parameters Optimization of the Proposed Weakly-Coupled FM-PCF

In this section, the main work is to find out the optimum geometrical parameters for the proposed weakly-coupled FM-PCF. We first obtain the approximate value of the design parameters based on the structural size of the conventional fiber and the simulation results. Then according to the result of simulation, we choose the optimized value for the proposed FM-PCF.

A. Optimization of Cladding Air Holes Parameters

Excessive confinement loss will cause excessive power attenuation, resulting in the inability of the signal to transmit. Therefore, confinement loss is what we must consider when analyzing the properties of photonic crystal fiber. Confinement loss (CL) can be obtained by the formula [15]:

$$CL = 8.086 k_0 Im(n_{eff}) \quad (2)$$

where $k_0 = 2\pi/\lambda$ is the wavenumber in vacuum, the Im(n_{eff}) is the imaginary part of effective refractive index, and the unit of CL is dB/km. The confinement loss strongly depends on fiber structure, and higher-order modes usually have more severe confinement losses. Therefore, we analyze the effect of the number of rings of air holes N on the confinement loss to obtain ultra-low confinement loss. From Fig. 2, we can find that the confinement loss decreases with N, and the confinement loss of ten vector modes (HE_{11a}, HE_{11b}, TM_{01}, HE_{21a}, HE_{21b}, TE_{01},

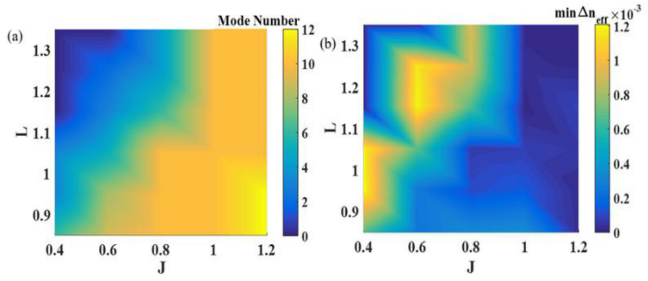

Fig. 3. Variation of (a)Mode number and (b)Minimum effective refractive index difference minΔn_{eff} as a function of L and J at $\lambda = 1550$ nm.

HE_{31a}, HE_{31b}, EH_{11a} and EH_{11b}) are all below $10-8$ when N is 6 or bigger, and the change of the confinement loss of each mode is relatively small. It should be noted that increasing the diameter of cladding by adding more rings of air holes could make the fiber vulnerable. Considering the manufacturing cost and calculation complexity, we take N = 6 for the proposed weakly-coupled FM-PCF which can support 10 vector modes and obtain ultra-low confinement loss ($<10^{-9}$ dB/km).

According to the preliminary optimization, we determine the initial parameters of the cladding air holes as $\Lambda = 2.95$ μm, d $= 1.8$ μm, $\Lambda_1 = 1.78$ μm and $d_1 = 1.33$ μm. And according to the equivalent refractive index method, the photonic crystal fiber can simulate as a step-index fiber, and the cladding area containing the air hole is approximated as the low-index cladding of the step-index fiber. Therefore, as the area of air hole with low refractive increases, the relative refractive index difference of the fiber with step index profile similar to the photonic crystal fiber will increase, and the number of propagation modes also increases. The different air holes distribution in the cladding adds extra freedom to the fiber design and consequently the control of fiber dispersion. We set the parameters L and J as scaling factors for the distance and the diameter of the inner and outer cladding air holes, respectively. We adjust distance and the diameter of the inner and outer cladding air holes in the same proportion to change the area of air hole with low refractive. Then, the influence of scaling factor L and J on mode number and minΔn_{eff} are shown in Fig. 3(a) and (b), respectively. It depicts that with the increase of L, the number of supporting modes decrease. And with the increase of J, the area of air hole with low refractive increase, so the relative refractive index difference of the fiber with step index profile similar to the photonic crystal fiber will increase, and the number of higher-order modes will increase. However, if the J is too large, the minΔn_{eff} between adjacent modes will decrease and cannot meet the condition of minΔn_{eff} $>10^{-4}$. When J = 0.8∼1 and L = 0.85∼0.95 μm, the proposed weakly-coupled PF-PCF can support 10 vector modes and can achieve large minΔn_{eff} ($>1 \times 10^{-4}$).

The chromatic dispersion is a significant parameter in optical fiber design. The chromatic dispersion of PCF can be easily calculated from the real part of the obtained effective refractive indices using following equation [26]:

$$D(\lambda) = -\frac{\lambda}{c}\frac{d^2 n_{eff}}{d\lambda^2}, \tag{3}$$

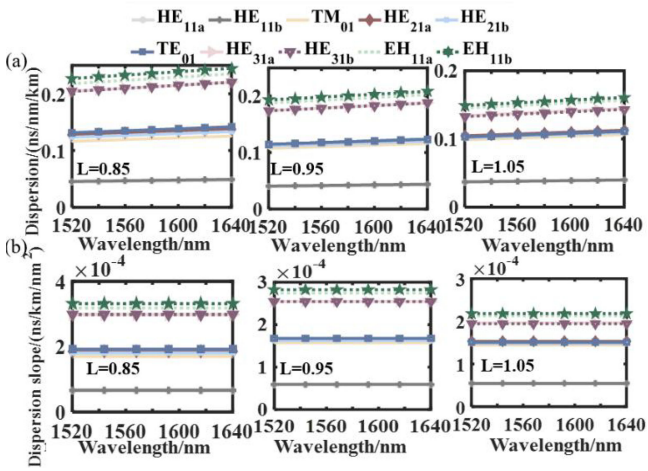

Fig. 4. Variation of (a)Chromatic dispersion and (b)Dispersion slope with wavelength for the scaling factor L of distance between air holes varying from 0.85 to 1.05.

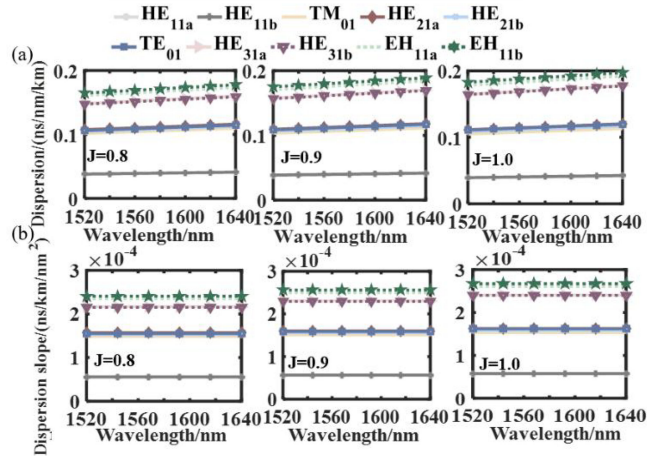

Fig. 5. Variation of chromatic dispersion (a) and chromatic dispersion slope (b) With wavelength for the scaling factor J of air holes diameter varying from 0.8 to 1.0.

where λ is operating wavelength and c is speed of light in vacuum. After calculating dispersion, we can also calculate dispersion slope with following equation:

$$S(\lambda) = \frac{dD(\lambda)}{d\lambda}, \tag{4}$$

Firstly, we study the influence of scaling factor L of pitch and scaling factor J of air holes diameters on chromatic dispersion. Fig. 4(a) and (b) depict the chromatic dispersion and dispersion slope versus wavelength with different values of scaling factor L of pitch. As it can be observed, with the increases of L, the distance between air holes increase, the chromatic dispersion and dispersion slope decreases. However, if the distance between air holes is too large, the number of modes supported by the fiber is reduced. In order to obtain flat dispersion and large minΔn_{eff} of 10 vector modes, we choose the point of L = 0.95, where $\Lambda =$ 2.8 μm, $\Lambda_1 = 1.7$ μm. And Fig. 5 shows that the dispersion and dispersion slope increase with the increases of scaling factor J of air holes diameter. The large minΔn_{eff} ($>1 \times 10^{-4}$) and flat

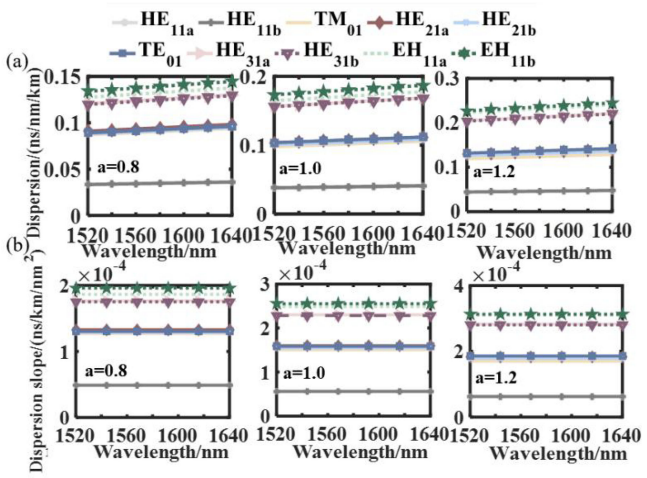

Fig. 6. Variation of chromatic dispersion (a) and chromatic dispersion slope (b) With wavelength for the diameter of first ring air holes a varying from 0.8 to 1.2 μm.

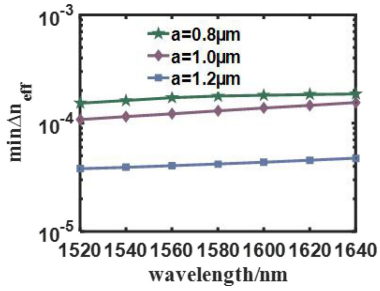

Fig. 7. Variation of $\min\Delta n_{eff}$ with wavelength for the a varying from 0.8 to 1.2 μm.

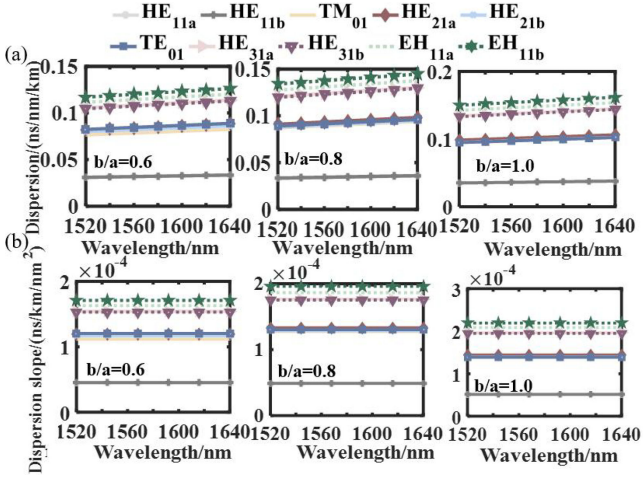

Fig. 8. Variation of chromatic dispersion (a) and chromatic dispersion slope (b) With wavelength for the ellipticity of first ring air holes b/a varying from 0.6 to 1.0.

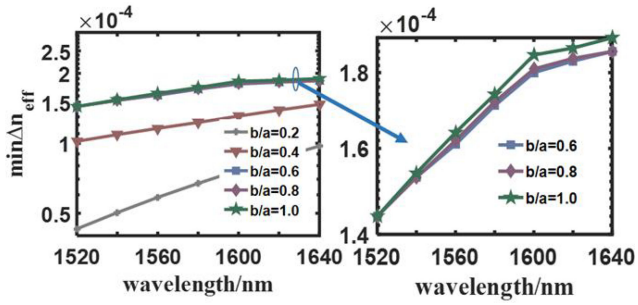

Fig. 9. Variation of with minΔneff wavelength for the ellipticity of first ring air holes b/a varying from 0.2 to 1.0.

chromatic dispersion can be achieved by choosing scaling factor of air holes diameter J = 0.8, where d = 1.57 μm, d_1 = 1.2 μm.

B. Optimization of First Ring Air Holes Parameters

Compared with the change of air hole in the outer rings, the change of the air holes in the first ring will directly affect the size of the defect area, and has the greatest impact on the dispersion characteristics of the proposed weakly-coupled FM-PCF. Firstly, only the air-hole diameter a in the first ring has been changed, while all the other geometric characteristics are kept constant to investigate the impact on chromatic dispersion and dispersion slope. It can be seen from Fig. 6 that when the diameter of first ring air holes increase, the chromatic dispersion and dispersion slope increase. Therefore, in order to get small and flat chromatic dispersion, the diameter of first ring air holes should not be too large. At the same time, we also considered the influence of the first ring air holes diameter on effective refractive index difference between adjacent modes. Fig. 7 shows the variation of $\min\Delta n_{eff}$ with wavelength in the range of a = 0.8∼1.2 μm, which depicts that with the increases of a, the $\min\Delta n_{eff}$ between adjacent modes decreases. And when a = 0.8∼1.0 μm, the $\min\Delta n_{eff} > 1 \times 10^{-4}$, so the large $\min\Delta n_{eff}$ and flat chromatic dispersion can be guaranteed.

We also investigate the influence of ellipticity of the first ring holes on chromatic dispersion and dispersion slope. As shown in Fig. 8, with the increase of b/a, the air holes of first ring are gradually rounded, and the dispersion and dispersion slope increase. Compared with the circular air holes (when b/a = 1.0), the elliptical structure of the first ring air holes can reduce the dispersion value and flat dispersion curve. In addition, we also analyze the effect of ellipticity on the effective refractive index difference between adjacent modes. It can be observed from Fig. 9, the elliptical structure of the first ring air holes cannot increase $\min\Delta n_{eff}$, and it decreases with the increase of ellipticity. And when b/a = 0.2, the $\min\Delta n_{eff} < 1 \times 10^{-4}$, which means that these modes cannot be transmitted independently. In order to flatten the dispersion and increase the Δn_{eff}, a balance should be found in the elliptical holes design, so we choose the ellipticity of first ring holes b/a = 0.6.

C. Optimization of Center Defected Air Hole Parameters

The rectangular air hole design in the center of the fiber can help to separate adjacent modes and increase the effective refractive index difference. Therefore, we first investigate the effect of center air hole diameter M, and the aspect ratio of the rectangle on $\min\Delta n_{eff}$ as shown in Fig. 10. It depicts that when

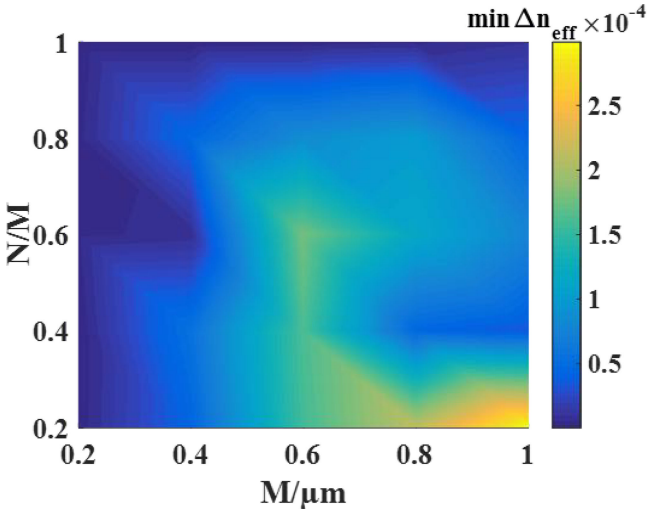

Fig. 10. Variation of minimum effective refractive index difference minΔneff as a function of the diameter M and aspect ratio N/M of the center rectangular defected air hole.

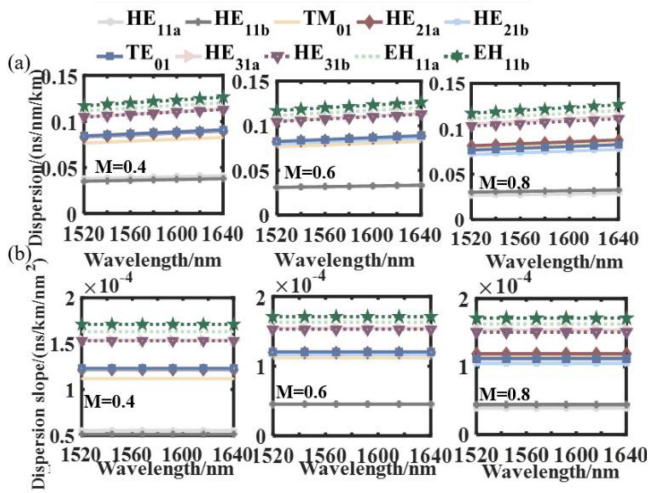

Fig. 11. Variation of chromatic dispersion (a) and chromatic dispersion slope (b) With wavelength for the diameter of center rectangular defected air hole varying from 0.4 to 0.8 μm.

the diameter of the air hole M is larger, the mode spacing is further separated, the value of minΔn_{eff} is larger, and the effect of the central air hole is more significant. And when the central defected air hole is a square, the minΔn_{eff} between adjacent modes is less than 10^{-4}, and as the aspect ratio of the central rectangular defected air hole increases, minΔn_{eff} can reach more than 10^{-4}.

The design of adding small holes in the center of the fiber also helps to flatten the dispersion. From the Fig. 11, we can see the influence of the increase of center defected rectangular air hole diameter M on the chromatic dispersion and dispersion slope. As the diameter M of the central air hole increases, the chromatic dispersion and dispersion slope decrease. At this time, the dispersion will be evenly distributed in the fiber cross-section structure, so it becomes more flatten. Because the design of the central small hole will cause certain energy loss, the hole

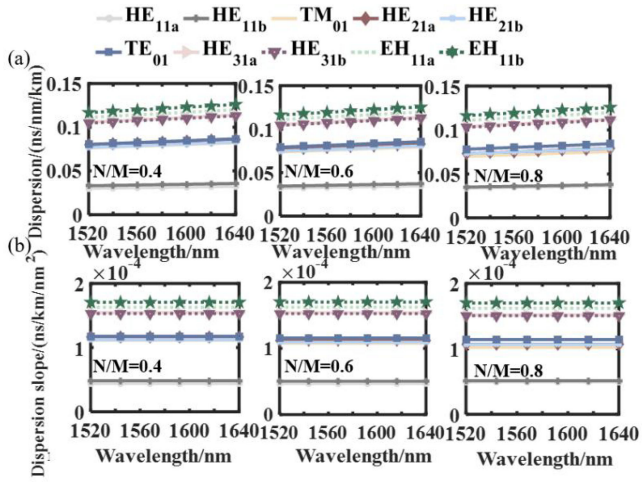

Fig. 12. Variation of chromatic dispersion (a) and chromatic dispersion slope (b) With wavelength for the aspect ratio of center rectangular defected air hole varying from 0.4 to 0.8.

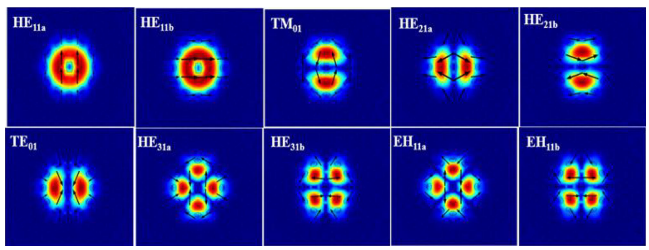

Fig. 13 Optical field intensity distributions of 10 vector modes in the proposed FM-PCF.

diameter should not be too large. The influence of the aspect ratio N/M of the central rectangular defected air hole on the chromatic dispersion and dispersion slope as shown in Fig. 12. It is clearly observed that, with the increase of the N/M, the chromatic dispersion and the dispersion slope decrease. The results show that a large N/M of central air hole is beneficial to the flattening of dispersion. In order to flatten the dispersion and increase the Δn_{eff} between adjacent modes, a balance should be found in the rectangular design. And when M = 0.6 μm and N/M = 0.4, the proposed weakly-coupled FM-PCF can obtain large minΔneff ($>1.6 \times 10^{-4}$) and flat chromatic dispersion (chromatic dispersion $<$0.13ns/nm/km, dispersion slope$<1.8 \times 10^{-4}$ ns/km/nm^2). Fig. 13 shows the optical field intensity distributions of 10 vector modes and the light is well confined in the core of the proposed weakly-coupled FM-PCF.

The final parameters of the proposed weakly-coupled FM-PCF are summarized in Table I. The chromatic dispersion of the target value is low than 0.15 ns/km/nm, and the chromatic dispersion slope of the target value is low than 1.8×10^{-4} ns/km/nm^2. The chromatic dispersion of lower than 0.2 ns/km/nm and the dispersion slope of lower than 1.8×10^{-4}ns/km/nm^2, can be realized for the tolerance scopes listed in Table I, indicating that the variations of all parameters maintain the negative flattened dispersion characteristics and that make the fabrication tolerance satisfied. And the bending in X and Y directions will not have a great impact on minΔn_{eff} between adjacent modes, chromatic

TABLE I
OPTIMAL PARAMETERS WITH FABRICATION TOLERANCE OF THE WEAKLY-COUPLED FM-PCF

	Tolerance range	Target value		Tolerance range	Target value
Λ [μm]	2.5-2.95	2.8	**a [μm]**	0.7-1.0	0.8
Λ_1 [μm]	1.53-1.8	1.7	**b/a**	0.4-1.0	0.8
d [μm]	1.44-1.8	1.57	**M [μm]**	0.4-0.8	0.6
d_1 [μm]	1-1.33	1.2	**N/M**	0.2-0.6	0.4

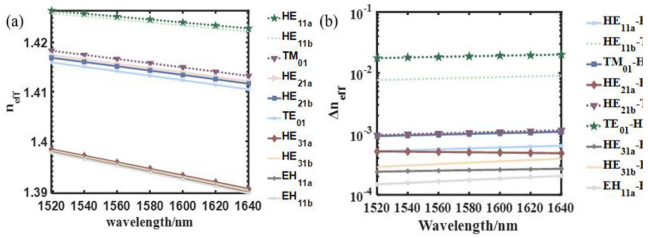

Fig. 14. Variation of n_{eff} (a) and Δn_{eff} (b) With wavelength.

dispersion and dispersion slope. Considering the realization of the desired fiber characteristics, the precise and well-established fabrication technology is also required because dimensional deviation has an impact on chromatic dispersion.

For short-haul transmission fibers, the coupling crosstalk between modes can be reduced by designing a larger effective refractive index difference. When the effective refractive index difference Δn_{eff} of each transmission mode in the fiber is larger than 10^{-4}, the crosstalk between the transmission modes can be reduced, thereby the mode crosstalk in the mode division multiplexing system can be effectively weakened or eliminated. [27] The variation of n_{eff} and Δn_{eff} with wavelength curve are shown in Fig. 14(a) and (b), respectively. It is observed that the minΔn_{eff} between adjacent modes of the proposed weakly-coupled FM-PCF is large than 1.6×10^{-4}, which indicates that the 10 vector modes can be independently transmitted.

IV. DIFFERENTIAL MODE DELAY

In short-haul transmission systems, MIMO-DSP can be simplified or eliminated when differential mode delay is low. Thus, the computation complexity and power consumption can be reduced. DMD between two modes is defined as the value of subtracting the group delay τ_A and τ_B, which is expressed as follows [28]:

$$\mathrm{DMD} = \tau_B - \tau_A = n_{gB} - n_{gA} = \frac{n_{effB} - n_{effA}}{c} - \frac{\lambda}{c}\left(\frac{\partial n_{effB}}{\partial \lambda} - \frac{\partial n_{effA}}{\partial \lambda}\right), \quad (5)$$

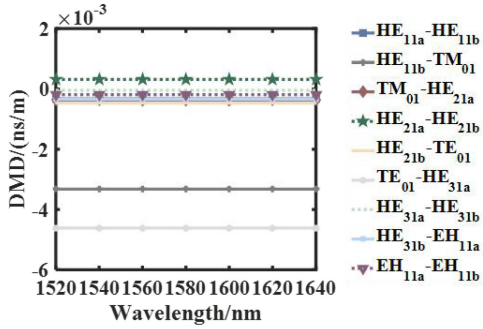

Fig. 15. Variation of DMD as a function of wavelength.

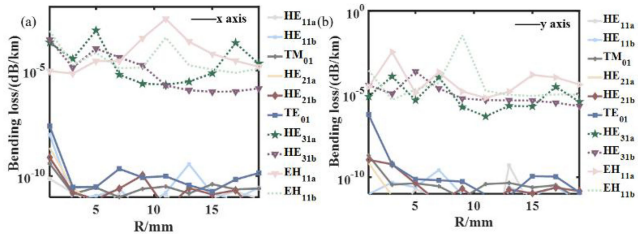

Fig. 16 Bending loss as a function of bending radius R along (a) x axis and (b) y axis.

where n_{gA} and n_{gB} are the group indices of mode A and B, c is the light velocity in a vacuum and λ means the free wavelength. Fig. 15 shows the variation of DMD as a function of wavelength. Calculated results of DMD for the proposed 10 modes weakly-coupled FM-PCF is from -5×10^{-3} to 0.5×10^{-3} ns/m, which can induce negligible power penalties in short-haul optical communication links.

V. BENDING LOSS ANALYSIS

Fiber bending influences the individual modes differently due to their mode felid distributions and propagation constants, and propagation modes that bear higher bending loss will distort and shift away from the center of the curvature. Therefore, the bending loss is very important for the analysis of fiber characteristics. The bending loss can be expressed by [29]:

$$BL = \frac{20}{\ln(10)} \frac{2\pi}{\lambda} Im(n_{eff}) \quad (6)$$

where Im(n_{eff}) means the imaginary part of n_{eff}. As shown in the Fig. 16(a) and (b), we analyzed the influence of bending radius in x and y directions on bending loss. It depicts that with the increases of bending radius R, the bending loss of propagation modes decrease, and the bending loss of higher-order modes is larger than low-order modes. When R is larger than 5 mm, the corresponding maximum bending losses of the first six modes along the x axis and y axis are smaller than 10^{-10} dB/km, which can be negligible. And when R>20 mm, the bending loss of the four higher-order modes along the x axis and y axis are around 10^{-5} dB/km. Simulation results show that the proposed weakly-coupled FM-PCF has strong resistance bending sensitivity.

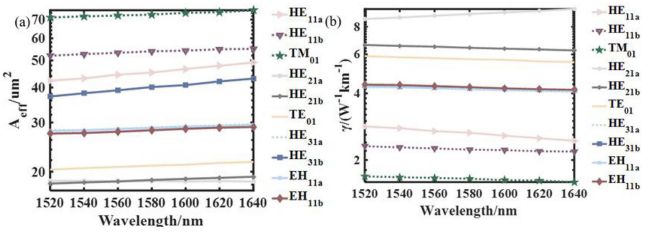

Fig. 17. Variation of effective area (a) and nonlinear coefficients γ(b) With wavelength.

VI. Effective Mode Area

The mode effective area (A_{eff}) is also one major parameter to decide fiber size. Large A_{eff} can limit the nonlinearity impairments in fiber transmission. We compute A_{eff} by [30]:

$$A_{eff} = \frac{\left[\int_{-\infty}^{+\infty} |E|^2 dxdy\right]^2}{\int_{-\infty}^{+\infty} |E|^4 dxdy}, \tag{7}$$

where E represents the mode field power distribution of the fiber cross section. Meanwhile, the nonlinearity coefficient γ (λ) of the PCF can be defined as formula (8) and the nonlinear coefficient in fibers are inversely proportional to A_{eff} [31],

$$\gamma(\lambda) = \frac{2\pi n_2}{\lambda A_{eff}}, \tag{8}$$

where $n_2 = 3.0 \times 10^{-20}$ m^2 w^{-1} is the nonlinear refractive index of silica. As shown in Fig. 17(a) and (b), we calculate effective area A_{eff} and nonlinear coefficients γ (λ) of the 10 propagate modes within the wavelength from 1520 nm to 1640 nm. As it can be observed from Fig. 17(a), the A_{eff} increases with the wavelength increases, and the effective area of 10 modes are larger than 18 μm^2. From Fig. 17(b), with the wavelength increases, the nonlinear coefficients of 10 vector modes decrease, the nonlinear coefficients γ of HE_{11a}, HE_{11b}, TM_{01}, HE_{21a}, HE_{21b}, TE_{01} HE_{31a}, HE_{31b}, EH_{11a}, EH_{11b} are smaller than 8w^{-1}km^{-1}.

The practical fabrication of the designed FM-PCF based on current fiber manufacture technologies is expected to be achievable. More recent technologies, such as extrusion and 3D printing, are demonstrated to fabricate different complex shaped asymmetrical air holes [32]. The extrusion technique developed by J. Wang et al. [33] offers fabrication freedom for complex structures including crystalline and amorphous PCFs. The sol-gel casting technique and in-situ polymerization demonstrated in [34], [35] offers the design freedom to fabricate micro-structured PCFs where air hole size and spacing can be adjusted independently, which can be anticipated that the verified techniques should be enough to fabricate small-sized elliptical and rectangular air holes the proposed structure. Therefore, we believe that the fabrication of the designed fiber is expected to be realized.

VII. Conclusion

In conclusion, the weakly-coupled ultra-flattened dispersion photonic crystal fiber supporting 10 vector modes (HE_{11a}, HE_{11b}, TM_{01}, HE_{21a}, HE_{21b}, TE_{01}, HE_{31a}, HE_{31b}, EH_{11a} and EH_{11b}) is proposed and investigated by numerical simulations. By using finite element method, we carry out numerical simulations to investigate the influence of design fiber parameters on Δn_{eff} and chromatic dispersion, and the ten vector modes of the proposed fiber satisfy the conditions that the effective refractive index difference is greater than 10^{-4} and the dispersion is flat. The ultra-flattened chromatic dispersion is achieved by introducing a small defected air hole in the center of core and the first ellipticity holes ring. The results show that the proposed fiber structure can achieve ultra-flattened chromatic dispersion (the dispersion slope$<1.8 \times 10^{-4}$ns/km/nm^2) and the effective refractive index of adjacent modes are larger than 1.6×10^{-4} in the wavelength range of 1520 nm to 1640 nm. The designed weakly-coupled FM-PCF supporting six vector modes also can achieve ultra-low confinement loss ($<10^{-9}$ dB/km) and low bending loss ($< 10^{-4}$ dB/km), which has the potential application for large-capacity MDM communication systems.

References

[1] A. B. Ani and M. Faisal, "Ultra-flattened broadband dispersion compensating photonic crystal fiber with ultra-low confinement loss," in *Proc. Int. Conf. Elect. Comput. Eng.*, 2016, pp. 243–246.
[2] T. A. Birks, J. C. Knight, and P. Russell, "Endlessly single-mode photonic crystal fiber," *Opt. Lett.*, vol. 22, no. 13, pp. 961–963, 1997.
[3] M. Delgado-Pinar, A. Diez, J. L. Cruz, and M. V. Andres, "High extinction-ratio polarizing endlessly single-mode photonic crystal fiber," *IEEE Photon. Technol. Lett.*, vol. 19, no. 8, pp. 562–564, Apr. 2007.
[4] M. Ebnali-Heidari, H. Saghaei, F. Koohi-Kamali, M. N. Moghadasi, and M. K. Moravvej-Farshi, "Proposal for supercontinuum generation by optofluidic infiltrated photonic crystal fibers," *IEEE J. Sel. Topics Quantum Electron.*, vol. 20, no. 5, Sep./Oct. 2014, Art. no. 7500408.
[5] W. Gao et al., "Numerical investigation on a new designed hollow-core photonic crystal fiber with large modal separation," *Opt. Quantum Electron.*, vol. 51, no. 11, pp. 1–8, 2019.
[6] K. Nyachionjeka, H. Tarus, and K. Langat, "Design of a photonic crystal fiber for optical communications application," *Sci. Afr.*. vol. 9, 2020, Art. no. e0051.
[7] T. A. Birks et al., "Endlessly single-modephotonic crystal fiber," *Opt. Lett.*, vol. 22, pp. 961–963, 1997.
[8] G. Agrawal, *Applications of Nonlinear Fiber Optics*. New York, NY, USA: Academic, 2010.
[9] J. Cho, X. Chen, and S. Chandrasekhar, "Trans-atlantic field trial using high spectral efficiency probabilistically shaped 64-QAM and single carrier real-time 250-Gb/s 16-QAM," *J. Lightw. Technol.*, vol. 36, no. 1, pp. 103–113, Jan. 2018.
[10] D. M. Spirit, A. D. Ellis, and P. E. Barnsley, "Optical time division multiplexing: Systems and networks," *IEEE Commun. Mag.*, vol. 32, no. 12, pp. 56–62, Dec. 1994.
[11] Z. M. Qiu and Y. S. Wong, "Dynamic workflow change in PDM systems," *Comput. Ind.*, vol. 58, no. 5, pp. 453–463, 2007.
[12] B. Mukherjee, "WDM optical communication networks: Progress and challenges," *IEEE J. Sel. Areas Commun.*, vol. 18, no. 10, pp. 1810–1824, Oct. 2000.
[13] A. Mecozzi and R.-J. Essiambre, "Nonlinear Shannon limit in pseudolinear coherent systems," *J. Lightw. Technol.*, vol. 30, no. 12, pp. 2011–2024, Jun. 2012.
[14] A. D. Ellis, J. Zhao, and D. Cotter, "Approaching the non-linear Shannon limit," *J. Lightw. Technol.*, vol. 28, no. 4, pp. 423–433, Feb. 2010.
[15] J. Wang, C. Jiang, W. Hu, and M. Gao, "Modified design of photonic crystal fibers with flattened dispersion," *Opt. Laser Technol.*, vol. 38, no. 3, pp. 169–172, 2006.
[16] X. L. Tan, Y. F. Geng, Z. Tian, P. Wang, and J. Q. Yao, "Study of ultraflattened dispersion square-lattice photonic crystal fiber with low confinement loss," *Optoelectron. Lett.*, vol. 5, no. 2, pp. 124–127, 2009.
[17] S. A. Razzak and Y. Namihira, "Proposal for highly nonlinear dispersion-flattened octagonal photonic crystal fibers," *IEEE Photon. Technol. Lett.*, vol. 20, no. 4, pp. 249–251, Feb. 2008.

[18] M. A. Islam and M. S. Alam, "Design optimization of equiangular spiral photonic crystal fiber for large negative flat dispersion and high birefringence," *J. Lightw. Technol.*, vol. 30, no. 22, pp. 3545–3551, Nov. 2012.
[19] Y. L. Hoo, W. Jin, J. Ju, H. L. Ho, and D. N. Wang, " Design of photonic crystal fibers with ultra-low, ultra-flattened chromatic dispersion," *Opt. Commun.*, vol. 242, pp. 327–332, 2004.
[20] R. Zeleny and M. Lucki, "Nearly zero dispersion-flattened photonic crystal fiber with fluorine-doped three-fold symmetry core," *Opt. Eng.*, vol. 52, no. 4, 2013, Art. no. 045003.
[21] T. Liang, W. Li, and G. Y. Feng, "Numerical simulation of supercontinuum generation in liquid-filled photonic crystal fibers with a normal flat dispersion profile," *Opt. Commun.*, vol. 343, pp. 196–202, 2015.
[22] Y. N. Zhang., "Optimization of highly nonlinear dispersion-flattened photonic crystal fiber for supercontinuum generation," *Chin. Phys. B*, vol. 22 no. 1, pp. 298–302, 2013.
[23] B. Wang, C. Jia, J. Yang, Z. Di, J. Yao, and J. Zhang, "Highly birefringent, low flattened dispersion photonic crystal fiber in the terahertz region," *IEEE Photon. J.*, vol. 13, no. 2, Apr. 2021, Art. no. 7200210.
[24] S. Wei-Hua, X. Chuan-Xiang, and Y. Jing, "A new type of few-mode photonic crystal fiber with nearly-zero flattened dispersion properties," in *Proc. 16th Int. Conf. Opt. Commun. Netw.*, 2017, pp. 1–3.
[25] H. Xiao, H. Li, B. Wu, Y. Dong, S. Xiao, and S. Jian, "Elliptical hollow-core optical fibers for polarization-maintaining few-mode guidance," *Opt. Fiber Technol.*, vol. 48, pp. 7–11, 2019.
[26] A. Medjouri, L. Simohamed, O. Ziane, and Z. B. Boudrioua, "Design of a circular photonic crystal fiber with flattened chromatic dispersion using a defected core and selectively reduced air holes: Application to supercontinuum generation at 1.55μm," *Photon. Nanostructures-Fundam. Appl.*, vol. 16, pp. 43–50, 2015.
[27] F. Yaman, N. Bai, B. Zhu, T. Wang, and G. Li, "Long distance transmission in few-mode fibers," *Opt. Exp.*, vol. 18, no. 12, pp. 13250–13257, 2010.
[28] R. Ryf et al., "Distributed Raman amplification based transmission over 1050-km few-mode fiber," in *Proc. Eur. Conf. Opt. Commun.*, 2015, pp. 1–3.
[29] Y. Tsuchida, K. Saitoh, and M. Koshiba, "Design and characterization of single-mode holey fibers with low bending losses," *Opt. Exp.*, vol. 13, no. 12, pp. 4770–4779, 2005.
[30] X. Wang, S. Lou, W. Lu, X. Sheng, T. Zhao, and P. Hua, "Bend resistant large mode area fiber with multi-trench in the core," *IEEE J. Sel. Topics Quantum Electron.*, vol. 22, no. 2, Mar./Apr. 2016, Art. no. 4400508.
[31] K. Saitoh and M. Koshiba, "Numerical modeling of photonic crystal fibers," *J. Lightw. Technol.*, vol. 23, no. 11, pp. 3580–3590, Nov. 2005.
[32] M. Islam, J. Sultana, and A. Dinovitser, "Zeonex-based asymmetrical terahertz photonic crystal fiber for multichannel communication and polarization maintaining applications," *Appl. Opt.*, vol. 57, pp. 666–672, 2018.
[33] T. Ma, A. Markov, L. Wang, and M. Skorobogatiy, "Graded index porous optical fibers-dispersion management in terahertz range," *Opt. Exp.*, vol. 23, pp. 7856–7869, 2015.
[34] Y. N. Zhang et al., "Casting preforms for microstructured polymer optical fiber fabrication," *Opt. Exp.*, vol. 14, pp. 5541–5547, 2006.
[35] J. Wang, X. H. Yang, and L. L. Wang, "Fabrication and experimental observation of monolithic multi-air-core fiber array for image transmission," *Opt. Exp.*, vol. 16, pp. 7703–7708, 2008.